Transient Heat Conduction through a Substrate of Brine-Spongy Ice

S.R. Dehghani[1], G.F. Naterer, Y.S. Muzychka

Department of Mechanical Engineering, Faculty of Engineering and Applied Science,

Memorial University of Newfoundland, St. John's, NL, A1B 3X5, Canada

Abstract

This paper develops a new predictive model of transient heat transfer in brine-spongy ice. It analyzes the thermal behavior and discusses the thermal response of brine-spongy ice to heat input. The model is based on the global characteristics of a mixture of ice and brine. The analytical model uses phase change characteristics of brine and ice in equilibrium states. The model involves a nonlinear partial differential equation and a number of equations of state for ice, brine, and brine-spongy ice. Salinity, initial temperature, and a constant temperature for one side of the ice block, are primary variables in the studies. Samples are also tested experimentally with transient conditions and their temperature responses are captured by a thermal camera. The numerical results are closely aligned with the measured temperatures. The experiments confirm the analytical model and numerical solutions. This paper establishes new understanding of trapped brine when absorbing and releasing thermal energy through brine-spongy ice. The observations indicate a new type of ice structure with considerable differences in thermal response to transient heat transfer as compared with regular ice.

Keywords: Brine-Spongy Ice, Transient Conduction, Latent Heat, Salinity, Phase Change

[1]Corresponding author, Postdoctoral Fellow, Phone: +1 (709) 771-6216, Email: srdehghani@mun.ca

23 **Nomenclature**

Variable	Unit	Definition
C_b	$\mathrm{J/(Kg.K)}$	Specific heat capacity of brine
C_e	$\mathrm{J/(Kg.K)}$	Equivalent specific heat capacity of brine-spongy ice
C_i	$\mathrm{J/(Kg.K)}$	Specific heat capacity of ice
C_s	$\mathrm{J/(Kg.K)}$	Specific heat capacity of brine-spongy ice
k_b	$\mathrm{W/(m.K)}$	Thermal conductivity of brine
k_i	$\mathrm{W/(m.K)}$	Thermal conductivity of ice
k_s	$\mathrm{W/(m.K)}$	Thermal conductivity of brine-spongy ice
L	m	Ice sample length
L_{Hb}	J/Kg	Latent heat of fusion of brine
Q_i	J/s	Input heat
Q_o	J/s	Output heat
Q_g'''	$\mathrm{J/m^3}$	Volumetric heat generation
$\dot{Q}_g'''$	$\mathrm{J/(m^3.}s)$	Rate of volumetric heat generation
S	%	Overall salinity
S_b	%	Salinity of brine
T	^{o}C	Temperature
T_s	^{o}C	Contact temperature
t	s	Time
t_0	s	Initial time
V_b	$\mathrm{m^3}$	Volume of brine in the element of brine-spongy ice
V_{Fb}	---	Volume fraction of brine

V_i	m^3	Volume of ice in the element of brine-spongy ice
α_{cb}	---	Coefficient of the equation of specific heat capacity of brine
α_{ci}	---	Coefficient of the equation of specific heat capacity of ice
α_{kb}	---	Coefficient of the equation of thermal conductivity of brine
α_{ki}	---	Coefficient of the equation of thermal conductivity of ice
α_{LHb}	---	Coefficient of the equation of latent heat of fusion of brine
α_{sb}	---	Coefficient of the equation of salinity of brine
$\alpha_{\rho b}$	---	Coefficient of the equation of density of brine
$\alpha_{\rho i}$	---	Coefficient of the equation of density of ice
V_s	m^3	Volume of the element of brine-spongy ice
dQ_g'''	J/m^3	Variation of volumetric heat generation
dt	s	Time interval
dV_{Fb}	---	Variation of volume fraction of brine
dV_i	m^3	Variation of volume of ice
ρ_b	Kg/m^3	Density of brine
ρ_e	Kg/m^3	Equivalent density of brine spongy ice
ρ_i	Kg/m^3	Density of ice
ρ_s	Kg/m^3	Density of brine spongy ice

1. Introduction

Icing of marine vessels, offshore structures, aircraft, overhead power lines, and wind turbines has been a serious challenge for many years (Panov, 1978; Zakrzewski and Lozowski, 1988; Lozowski et al., 2000). Ice accretion on marine vessels can cause many difficulties and hazardous situations

(Ryerson, 2011). The type and amount of accumulated ice on marine vessels greatly depend on the seawater temperature, wind speed, wind temperature, marine object geometry and velocity, seawater salinity and other known and unknown parameters (Kulyakhtin and Tsarau, 2014; Gates et al. 1986; Lozowski et al., 2000).

Although various situations of icing phenomena lead to the creation of different types and structures of ice, it is known that some brine is always trapped between the solid ice structures during the icing phenomena and consequently makes a unique blend of ice and brine (Gates et al., 1986; Makkonen, 1987; Makkonen, 1990). This type of ice, in this paper, is called *brine-spongy ice*. When a portion of salty water starts to freeze, it rejects the dissolved salt, and as a result, pure ice in the vicinity of the brine is created (Weeks and Ackley, 1982; Shakeel, 1987). In many cases, the pure ice is developed by growth of dendritic ice (Glicksman, 2011). This type of ice formation increases the likelihood of trapping brine between the dendrites (Shakeel, 1987; Glicksman, 2011). During the icing, a small amount of brine is trapped between the pure ice structures. This mixture of ice and trapped brine is created layer by layer, and in fact the brine-spongy-ice accretion mechanism holds the main role in icing marine vessels (Panov, 1978; Gates et al., 1986; Makkonen 1990).

The state of equilibrium between brine and ice depends on the salinity of the brine pockets and the local temperature (Weeks and Ackley, 1982; Shakeel, 1987). Increasing or decreasing the salinity of the brine pockets causes melting and icing respectively (Weeks, 2010). In addition, varying the temperature moves the state of equilibrium toward melting or icing (Shakeel, 1987; Weeks, 2010). As spongy ice loses heat and becomes colder, the volume of trapped brine decreases and that of pure ice is increased (Shakeel, 1987). Due to the decrease in temperature, the salt is rejected into the brine pockets and the salinity of the brine pockets increases (Weeks and Ackley,

1982; Shakeel, 1987; Weeks, 2010). Decreasing salinity and temperature create a new state of equilibrium for ice and brine in a brine-spongy ice medium (Shakeel, 1987; Blackmore and Lozowski, 1998).

The brine-spongy ice usually experiences various contact temperatures and heat transfer conditions (Panov, 1978; Gates et al., 1986; Lozowski et al., 1996.). Due to the trapped brine inside the ice cavity, the transient thermal behavior of brine-spongy ice is not solely heat conduction; phase change plays a significant role (Blackmore and Lozowski, 1998). The freezing temperature of trapped brine depends on its local salinity (Shakeel, 1987; Weeks and Ackley, 1982). The freezing point of pure water is close to zero degrees Celsius and it decreases as the salinity increases. The other thermo-physical properties of brine pockets are functions of salinity and temperature (Shakeel, 1987).

The transient thermal behavior of brine-spongy ice has not been well understood in the literature. The trapped brine in the ice structure can cause significant changes in the response of this medium to transient heat transfer (Shakeel, 1987). In this study, analytical models of heat transfer for brine-spongy ice are developed including with a numerical scheme, which is based on a finite difference method. An experimental test rig is also used to conduct the relevant experiments for verification of the analytical model and numerical results.

2. Heat Transfer Formulation

The thermal behavior of brine-spongy ice is strongly dependent on its overall salinity and local temperature (Shakeel, 1987; Weeks and Ackley, 1982). In brine-spongy ice, the higher overall salinity and temperature result in higher amounts of trapped brine ice and consequently the thermal

behavior closer to the brine. On the other hand, a lower temperature and lower overall salinity lead to conditions similar to a solid-ice-salt condition (Makkonen, 1987; Macklin and Ryan, 1962).

The variable freezing point and heat of fusion of trapped brine in brine-spongy ice create a complicated ice-brine region that can affect the thermal behavior of a block of brine-spongy ice (Blackmore et al., 2002; Blackmore and Lozowski, 2003; Lozowski et al., 2005). Figure 1 shows a schematic view of brine-spongy ice. The brine pockets are confined by pure ice. Pure ice and brine pockets are in a local equilibrium state. The salinity of a brine pocket is directly dependent on its local temperature. This means by increasing the temperature, some pure ice is melted and the salinity of brine pockets is decreased, and vice versa.

Steady state heat transfer in pure ice and brine-spongy ice transfers the sensible heat energy across the region (Weeks and Ackley, 1982). In the case of transient heat transfer, the behaviors are different. The heat transfer in pure ice is again limited to transferring sensible heat, but for brine-spongy ice, the heat of fusion has an important role. In brine-spongy ice, thermal energy cannot pass through the media exclusively as sensible heat (Shakeel, 1987; Weeks and Ackley, 1982). The passage of heat affects the local temperature of brine-spongy ice and consequently, some small amounts of ice melt and join the brine pockets and vice versa.

Figure 2 illustrates a brine-spongy ice medium which is affected by a sudden flux of heat from the left side for a defined period. Once heating is started, thermal energy moves from the higher temperature toward the lower temperature region, which is the right side of the medium. This causes an increase in the temperature of the ice and brine pockets in its path. Increasing the temperature of brine pockets and ice creates a new state of equilibrium and consequently, part of the ice is melted and joined to its neighbor brine pockets. In this circumstance, the volume of brine pockets is increased and the volume of ice is decreased. As a result, the volume fraction of brine,

which is the ratio of volume of brine pockets to ice volume, is increased (Shakeel, 1987; Weeks and Ackley, 1982). After a short time, heat affects part of this medium, which is named the heated zone. In this zone the brine pockets have become larger than those of the unheated zone. The thermal energy cannot pass through any section of brine-spongy ice without melting or solidifying of a small portion of the ice or brine. This means some part of the transient thermal energy is absorbed in heating the local medium including ice and brine pockets, and some part is absorbed in melting a small amount of ice, while the rest can pass through, and vice versa. Figure 3 shows differences in the energy passage and storage in a segment of brine-spongy ice and pure ice which are affected by the heat input.

The governing equations for heat transfer in brine-spongy ice media can be derived by considering a small element of brine-spongy ice. Figure 4 shows a small element of brine-spongy ice at an initial time of $t = t_0$ and after a short time of dt, t=$t_0 + dt$. The element contains a brine pocket which is confined by pure ice. After a short time, and due to entering heat, some ice is melted and it joins the brine pocket. Therefore the volume of the brine pocket is increased and the volume of pure ice is decreased. The salinity of the brine pocket is decreased because of the addition of new melted ice to it. The brine and ice absorb sensible heat and as a result their temperatures are higher. The heat of fusion for melting ice is the other part of the heat exchange. The rest of the heat input passes through the element and exits from the other sides.

The rate of volumetric heat generation in the element can be calculated from the density of ice, the melted ice volume, the heat of fusion of brine, and the volume of the element. The generated heat which is a result of phase change depends on the amount of phase change. Eq. (1) shows the rate of volumetric heat generation in a short period of time.

$$\frac{dQ_g'''}{dt} = \frac{-\rho_i \, dV_i \, L_{Hb}}{V_s \, dt} \tag{1}$$

120 The volume fraction of brine is $V_{Fb} = V_b/V_s$. TBy using the derivative of V_{Fb} and Eq. (1),
121 the rate of volumetric heat generation in an element of brine-spongy ice can be obtained.

122 $$\frac{dQ_g'''}{dt} = \rho_i \, L_{Hb} \, \frac{dV_{Fb}}{dt} \tag{2}$$

123 $$\dot{Q}_g''' = \rho_i \, L_{Hb} \, \frac{\partial V_{Fb}}{\partial t} \tag{3}$$

124 Eq. (3) shows the amount of volumetric heat generation in an element of brine-spongy ice due to
125 the time variation of volume fraction of brine in the element. By knowing the overall salinity of
126 the spongy ice, the volume fraction of brine can be calculated for each temperature. Eq. (4) is an
127 empirical relation that calculates the volume fraction for any temperature and overall salinity
128 (Weeks and Ackley, 1982; Weeks 2010).

129 $$V_{Fb} = 10^{-3} \, S \, (-\frac{49.185}{T} + 0.532) \tag{4}$$

130 By using Eq. (3) and Eq. (4), a new relation for heat generation, which is dependent on the overall
131 salinity, temperature, and time variation of temperature, is obtained.

132 The governing equation for transient heat transfer (Ozisik, 1993) with heat generation is

133 $$\rho_s \, C_s \frac{\partial T}{\partial t} = \vec{\nabla}.\left(k_s \, \vec{\nabla} T\right) + \dot{Q}_g''' \tag{5}$$

134 Eq. (5), which is a heat conduction equation for a medium with a moving heat source, can be used
135 as a governing equation for heat transfer in brine-spongy ice. The interface of phase change acts
136 as a moving heat source. Melting absorbs the latent heat of fusion, and icing releases the latent
137 heat of fusion. The volumetric rate of heat generation of the phase change is calculated by the
138 derivative of V_{Fb}. Using this equation and replacing $\dot{Q}_g'''$ in Eq. (5), the governing equation of heat
139 transfer in a brine-spongy ice is obtained as follows:

140 $$\rho_e \, C_e = \left(\rho_s \, C_s - \frac{\rho_i \, L_{Hb} \, S \, 49.185 \times 10^{-3}}{T^2}\right) \tag{6}$$

141 $$\rho_e \, C_e \frac{\partial T}{\partial t} = \vec{\nabla}.\left(k_s \, \vec{\nabla} T\right) \tag{7}$$

This partial differential equation is dependent on overall salinity and thermal properties of brine pockets, ice, and brine-spongy ice. Table 1 shows relations which describe the thermal properties of ice, brine, and brine-spongy ice (Weeks and Ackley, 1982; Weeks 2010; Cox and Weeks 1975).

Eq. (4), Eq. (7), and the equations of properties in Table 1 yield 13 equations and 13 unknowns leading to a set of nonlinear equations. The unknowns are temperature, brine conductivity, brine heat capacity, brine salinity, brine density, brine heat of fusion, ice density, ice thermal conductivity, ice heat capacity, spongy ice conductivity, spongy ice density, spongy ice heat capacity, and volume fraction of brine. Properties of spongy ice are considered as weighted properties of ice and brine. The properties in Table 1 are empirical relations of previous investigators (Weeks and Ackley, 1982; Weeks 2010; Cox and Weeks 1975). These are dependent on the coefficients which are obtained experimentally. Table 2 includes the coefficients in the equations of Table 1 (Weeks and Ackley, 1982; Weeks 2010; Cox and Weeks, 1975). With an initial condition, which is the initial distribution of temperature in the brine-spongy ice, the boundary conditions, and also the overall salinity of brine-spongy ice, this set of 13 equations and 13 unknowns can be solved. The results will predict the thermal behavior of brine-spongy ice at each moment of time.

3. Experimental Investigation

A cold plate, for which the coolant is supplied from a cold bath containing a mixture of water and glycol, maintains a wide range of low temperatures from zero to $-25^{o}\mathrm{C}$. The cooling capacity of the cold plate is enough to maintain the temperature at a set point. A cold bath, which is filled with a glycol-water mixture, supplies the chilled liquid for the cold plate. A thermal camera, which is calibrated for subzero temperatures with an accuracy of ±0.1 ^{o}C measures the temperatures of

target points and areas. The experiments are conducted with a cold plate which is adjusted to a set point equal to the initial temperature of a block of brine-spongy ice. The size of the samples and the magnitude of the heat transfer between the samples and the cold plate are such that the cold plate can accurately maintain a set temperature during the experiments. The cold plate keeps one side of the ice samples at a chosen temperature between $-5^{o}\mathrm{C}$ and $-20^{o}\mathrm{C}$. Figure 5 illustrates the experimental setup and the most significant elements involved in the experiments.

Various samples with different salinities are created and kept in a freezer, equipped with a temperature controller, to reach the desired temperature. A uniform temperature is established throughout the ice. The experimental tests are conducted by using salinities between zero and 65%, a fixed initial temperature, which is $-20^{o}\mathrm{C}$, and a fixed temperature for the cold plate which is $-5^{o}\mathrm{C}$. The main measured parameter is the variation of the end temperature of the ice block over time. The variation of temperature over time can confirm the role of brine pockets in the thermal behavior of brine-spongy ice.

The samples are made by mixing water and appropriate amounts of salt. The saline samples are placed in small containers and placed in a freezer with the target initial temperatures. Mixing and shaking of the containers during freezing aids in the creation of the homogeneous brine-spongy ice. The samples are kept at $-20^{o}C$ for about a day. They are then brought out of the containers and kept for another day at $-20^{o}\mathrm{C}$. At this point they are ready for the experiments. The cold plate maintains the contact temperatures and the samples are placed directly on the cold plate. The thermal camera starts to capture the temperatures of the end side of the ice blocks.

4. Results and Discussion

The governing equations of brine-spongy ice are solved for obtaining the transient heat transfer in brine-spongy ice in different situations. A one-dimensional case is considered. Figure 6 shows a Cartesian one-dimensional problem of transient heat transfer in brine-spongy ice. The right- side of the medium experiences a thermally isolated condition, and the left- side has a constant-temperature condition, T_s. The overall salinity and initial temperature, which is a constant temperature throughout the ice, are known. The sizes of brine pockets are not significant in comparison to the length scale of brine-spongy ice. Homogeneous small pockets of trapped brine make an almost uniform blend of ice and brine medium.

The governing equations for different cases of brine-spongy ice media with various initial and boundary conditions are solved and the results are compared and discussed. Overall salinity can change the state of equilibrium significantly; increasing the volume of trapped brine, which occurs because of increasing overall salinity, is one of the expected results of examining the brine-spongy ice media.

As discussed, the main outstanding feature of brine-spongy ice appears in transient situations. In these circumstances, the contribution of brine pockets in generation, absorption, and transfer of heat is significant. An investigated parameter is the thermal response of brine-spongy ice to time. In this case, the initial temperature of brine-spongy ice is considered $-20^{o}\mathrm{C}$, and the left side of the ice block, T_s, is kept at a constant temperature of $-5^{o}\mathrm{C}$. The ice thickness is 20 mm. Figure 7 shows the thermal response of brine-spongy ice to a transient problem during the time of $\mathrm{t} = 0$ s to $\mathrm{t} = 300$ s.

The warmer side of the ice block, the left side, affects the spongy ice and starts to transfer heat inside the ice. The heat penetrates the spongy ice from the left side of the block, and a portion of ice which is closest to the left side, is affected by the heat immediately. Figure 7 shows the

profiles of temperature across the spongy ice at various moments of time. As penetration of the heat into the spongy ice is increased, the spongy ice becomes warmer. The temperature variation in the block of spongy ice shows that after one second only 15% of the medium is affected by the heat input. The remaining 85% is unheated at this time. The penetration of heat is increased by increasing the time; at $\mathrm{t} = 15$ s the heated zone is about 50% of the medium. After about 60 s the whole medium is heated. At this time the right-side temperature is approximately equal to the initial temperature of the medium. At $\mathrm{t} = 180$ s and $\mathrm{t} = 300$ s, the penetrated heat increases the right-side temperatures to $-17^{o}\mathrm{C}$ and $-15^{o}\mathrm{C}$ respectively.

As the brine-spongy ice becomes warmer, the state of equilibrium between the brine pockets and the ice shifts to melt more ice. The melted ice is added to the brine pockets and as a result the salinity of the brine pockets is decreased. Figure 8 shows that after one second, the salinity of brine pockets in the 15% heated zone is decreased. The minimum salinity of brine pockets in the whole region, which occurs at the left side, is about 80%, which is considerably less than the initial salinity of brine pockets, which is about 225%. As time passes, the heat penetrates more and the heated zone is increased, the melted ice is increased, and consequently the salinity of the brine pockets decreases. The salinity of the brine pockets on the right side will be about 190% after 300 s.

Melting the ice and joining the melted ice with the brine pockets can increase the volume of the brine pockets and reduce the volume of ice and consequently, the volume fraction of brine is increased. Figure 9 shows that as time increases, the volume fraction of brine is increased. The maximum volume fraction of brine, which occurs on the left side, is about 0.67. This means 67% of the volume of brine-spongy ice at this point is occupied by brine pockets. The rest of the volume

is occupied by the ice. The initial volume fraction of the brine is about 19%, and after a short time and in accordance with the amount of heat absorption, it can be increased to higher values.

The amount of dissolved salt in the water plays an important role in the thermal behavior of brine-spongy ice. Increasing the overall salinity changes the state of equilibrium toward freezing the ice at a lower temperature. Figure 10 shows the thermal response of the brine-spongy ice to various salinities. The numerical solutions are conducted in situations of an initial condition of $-20^{o}\mathrm{C}$, and a boundary condition of $-5^{o}\mathrm{C}$. In addition, the overall salinity can vary between zero and 65%. The results are given for $\mathrm{t} = 300$ s.

As Fig. 10 shows that the pure ice is greatly affected by the boundary condition, $\mathrm{T} = -5^{o}\mathrm{C}$. After 300 s the temperature of the pure ice is increased from $-20^{o}\mathrm{C}$ to a range of $-7^{o}\mathrm{C}$ to $-5^{o}\mathrm{C}$. The responses of high-saline cases, however, are completely different. For the high-salinity ice, the temperature is between $-15^{o}\mathrm{C}$ and $-5^{o}\mathrm{C}$. This means the temperature across the high-salinity ice is affected by the boundary less than that of the pure ice. This occurs because of the contribution of the brine pockets in the process of heat storage inside the brine-spongy ice. Some heat is stored in the brine pockets by melting the ice, and as a result the sensible heat cannot increase the temperature of the medium significantly.

As the model predicts, increasing the overall salinity increases the salinity of brine pockets. Figure 11 confirms that the salinity of the brine pockets for an overall salinity of 65% can be up to 190%. In this case the salinity of the brine pockets for an overall salinity of 5% cannot be more than 120%. The salinity of brine pockets which is closer to the left side is less than that of the right side. The warmer side melts more ice and therefore decreases the salinity of its vicinity brine pockets.

The other interesting fact is the volume fraction of brine. In Fig. 12, by increasing the overall salinity, the volume fraction of the brine increases. For the left side, which is affected by the heat input, this variation is more considerable. The brine volume fraction of the pure ice is zero, as expected. The highest volume fraction of brine occurs in the highest overall salinity case, which is the case of an overall salinity of 65%. In this case, the volume fraction of brine can be up to 0.67. This means that about 67% of the brine-spongy ice is occupied by the brine pockets in the left-side.

The heat input from the left-side is caused by the high temperature of the left-side boundary condition, which is a contact temperature. This temperature is high in comparison to the initial temperature of the medium. The thermal responses for a block of brine-spongy ice, which is affected by various contact temperatures, has a length of 20 mm, an overall salinity of 65%, and an initial temperature of $-20^{o}\mathrm{C}$. Figure 13 shows the thermal responses of this medium for different contact temperatures from $-5^{o}\mathrm{C}$ to $-20^{o}\mathrm{C}$.

For a contact temperature of $-20^{o}\mathrm{C}$, the temperature of the ice and the contact temperature are the same and they are in a thermal equilibrium. Therefore, no heat transfer or changes in the ice are expected. As differences between the contact temperature and the initial temperature of the ice are increased, the rate of heat input increases and consequently the changes in the brine-spongy ice appear. The most affected case is that of the contact temperature of $-5^{o}\mathrm{C}$. In this case, the right- side temperature, the insulated side, reaches $-15^{o}\mathrm{C}$, while the right- side temperature in the case of $-15^{o}\mathrm{C}$ is about $-18^{o}\mathrm{C}$.

As with other cases, the greatest change in salinity of the brine pockets is the case with the maximum heat input. For the case of a contact temperature of $-5^{o}\mathrm{C}$, the salinity of brine pockets reduces to 80% and the volume fraction of the brine goes up to 0.67. These changes are less for

277 the cases with lower contact temperatures. Figure 14 shows the variation of salinity of brine
278 pockets in various contact temperatures.

279 The insulated side is also affected by the variation of right- side temperatures. After 300 s,
280 the minimum salinity of the brine pockets occurs for the highest contact temperature. It is about
281 180% in the right- side. Higher contact temperature melts more ice and consequently increases the
282 volume fraction of the brine pockets in the warmer regions. Figure 15 shows the effects of
283 increasing of volume fraction of brine in various contact temperatures. The right-side, which is not
284 affected by heating after 300 s, has less variation of volume fraction.

285 The initial temperature of brine-spongy ice is the other important factor in the thermal
286 behavior of this ice. A lower initial temperature can cause trapped brine with a higher level of
287 salinity and a lower volume fraction. As the initial temperature increases, the brine-spongy ice will
288 contain a lower level of salinity of brine pockets and a higher volume fraction. Figure 16 shows
289 the thermal response of brine-spongy ice at some different initial temperatures. The solutions are
290 presented for an overall salinity of 65% and the results are given for t=300s. The initial temperature
291 of $-20^{o}\mathrm{C}$ causes the lowest temperature in the right-hand side. The higher initial temperatures will
292 result in a higher temperature in the right-hand side.

293 The salinity of brine pockets, which is a function of temperature, is affected by initial
294 temperatures. The highest salinity corresponds to the lowest initial temperature. Because the right-
295 side is cooler than the left-side, the salinity of brine pockets in the right-hand side is more than that
296 of the left-side. Figure 17 shows the variation of salinity of brine pockets at various initial
297 temperatures.

298 The changes in the salinity of the brine pockets and the volume fraction of the brine are
299 related to each other. They experience higher variations with an initial temperature of $-20^{o}\mathrm{C}$. The

other initial temperatures create some changes in the temperature, salinity of brine pockets, and volume fraction of brine as well. As a common result, the higher initial temperatures cause less changes in the temperature, salinity of brine pockets, and brine volume fraction. Figure 18 shows the variation of volume fraction of brine at various initial temperatures. The lowest volume fraction occurs for the coldest points, which are the right-side. The volume fraction in the case of $-20^{o}\mathrm{C}$ remains the minimum volume fraction in the whole medium.

The experimental tests are performed for various overall salinities. The overall salinities are varied from zero, for fresh water, to 65%. Figure 19 shows a comparison between the measured temperatures and the numerical results. The numerical results for fresh water are in good agreement with the experimental results. The measured temperatures are a little lower than the numerical results. This occurs because of small trapped air bubbles in the ice. As the overall salinity increases, the brine-spongy ice is less affected by the heat input. The error is lowest for the highest overall salinity. In this case the error is about 5%. The measured temperatures are again lower than the numerical results. The errors may occur because of the thermo-physical properties of brine and ice, trapped air bubbles, numerical solutions and also temperature measurements by the thermal camera. The experimental results provide useful validation of the numerical solution. The maximum error is about 5%.

5. Conclusions

A new predictive model of transient heat transfer in brine-spongy ice was developed. This model was obtained by assuming a homogeneous distribution of small brine pockets in brine-spongy ice. The properties of pure ice, brine pockets and a mixture of ice and brine are used to address the properties of brine-spongy ice. The contribution of melting and solidification of ice and brine

pockets leads to a sensible-latent heat transfer process through the brine-spongy ice. A numerical method is used to solve the governing equations. The numerical solutions show that brine-spongy ice is less impacted by the heat input than pure ice. The temperature of the end point of a sample of brine-spongy ice varies by about $5^{o}\mathrm{C}$, while in the same situation the end point of pure ice varies by about $13^{o}\mathrm{C}$. Brine pockets absorb a portion of the heat input by melting the surrounding ice. Melted ice increases the volume fraction of brine and consequently the salinity of brine pockets is decreased. Also, an experimental setup using a calibrated thermal camera measures the end point temperature of the block of brine-spongy ice. The experimental results provide useful validation of the predictive model. The measured temperatures are less than 5% lower than the numerical results.

Acknowledgments

The authors gratefully acknowledge the financial support of Statoil (Norway), MITACS, and Petroleum Research Newfoundland and Labrador (PRNL) for this research.

References

Blackmore, R.Z., Lozowski, E.P., 1998. A theoretical spongy spray icing model with surficial structure. Atmospheric Research, 49(4), 267–288.

Blackmore, R.Z., Lozowski, E.P., 2003. Spongy icing modelling: Progress and prospects. The Thirteenth International Offshore and Polar Engineering Conference, 25-30 May, Honolulu, Hawaii, USA.

Blackmore, R.Z., Makkonen, L., Lozowski E.P., 2002. A new model of spongy icing from first principles. Journal of Geophysical Research, 107(D21), AAC 9-1-AAC 9-15.

346 Cox, C.F.N., Weeks, W.F., 1975. Brine drainage and initial salt entrapment in sodium chloride
347 ice. U.S. Army Cold Regions Research and Engineering Laboratory, Research Report 345.
348 Gates, E.M., Narten, R., Lozowski, E.P., Makkonen, L., 1986. Marine icing and spongy ice. IAHR
349 Ice Symposium, 153-163.
350 Glicksman, M.E., 2011. Mechanism of dendritic branching. Metallurgical and Materials
351 Transactions A, 43(2), 391-404.
352 Kulyakhtin, A., Tsarau, A., 2014. A time-dependent model of marine icing with application of
353 computational fluid dynamics. Cold Regions Science and Technology, 104–105, 33–44.
354 Lozowski, E.P., Blackmore, R.Z., Forest, T.W., Shi, J., 1996. Spongy icing in the marine
355 environment. OMAE, Volume IV, 55-61.
356 Lozowski, E.P., Oleskiw, M., Blackmore, R.Z., Karev, A., Kolar, L., Farzaneh, M., 2005. Spongy
357 Icing Revisited: Measurements of Ice Accretion Liquid Fraction in Two Icing Tunnels. 43rd AIAA
358 Aerospace Sciences Meeting and Exhibit, Aerospace Sciences Meetings.
359 Lozowski, E.P., Szilder, K., Makkonen, L., 2000. Computer simulation of marine ice accretion.
360 Royal Society, 358, 2811-2845.
361 Macklin, W.C., Ryan, B.F., 1962. On the formation of spongy ice. Quarterly Journal of the Royal
362 Meteorological Society, 88(378), 548–549.
363 Makkonen, L., 1987. Salinity and growth rate of ice formed by sea spray. Cold Region Science
364 and Technology, 14, 163-171.
365 Makkonen, L., 1990. The origin of spongy ice. IAHR Ice Symposium, 1022-1030.
366 Ozisik, M.N., 1993. Heat Conduction. John Wiley & sons, Inc.
367 Panov, V.V., 1978. Icing of Ships. Polar Geography, 2 (3), 166-186.

Ryerson, C.C., 2011. Ice protection of offshore platforms. Cold Regions Science and Technology, 65 (1), 97–110.

Shakeel, T., 1987. Dynamics of spontaneous pattern formation in dendritic ice crystal growth. PhD Thesis, State University of New York.

Zakrzewski, W.P., Lozowski, E.P., 1988. Estimating the extent of the spraying zone on a sea-going ship. Ocean Engineering, 15(5), 413–429.

Weeks, W.F., 2010. On sea ice. University of Alaska Press.

Weeks, W.F., Ackley, S.F., 1982. The growth, structure, and properties of sea ice. CRREL Monograph 82-1.

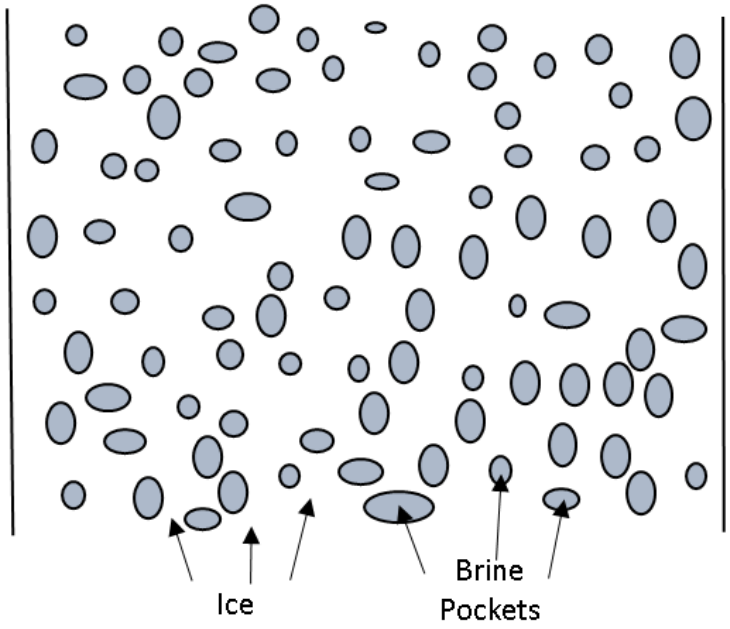

Fig. 1. Schematic of brine-spongy ice

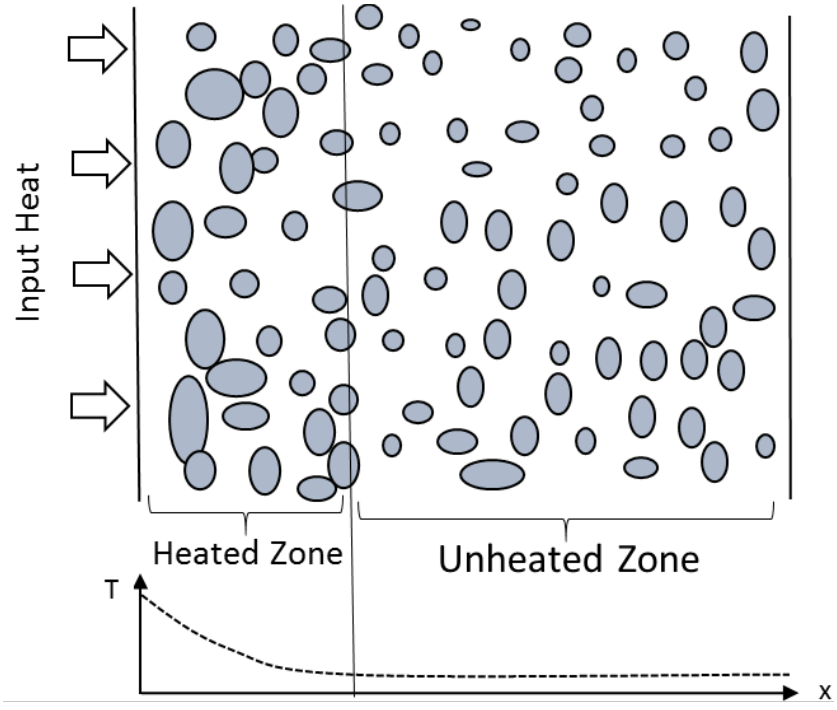

Fig. 2. Thermal response of brine-spongy ice to transient heat input

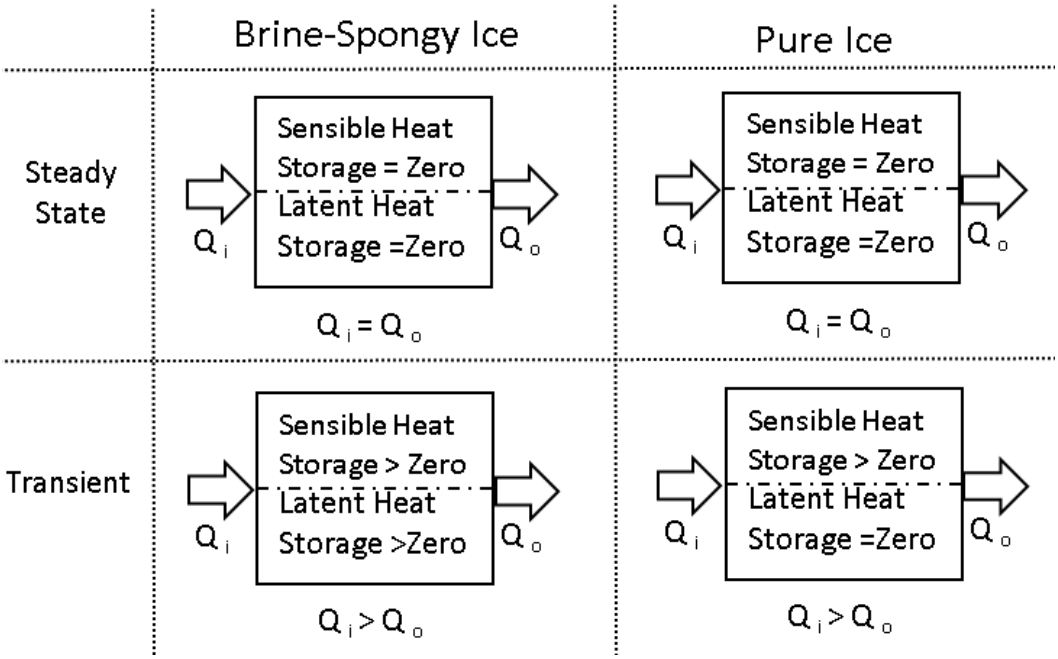

Fig. 3. Sensible and latent heat storage in brine-spongy and pure ice

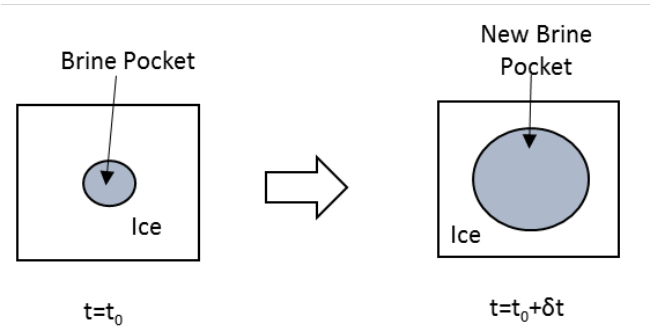

Fig. 4. Small element of brine-spongy ice in a finite period of time

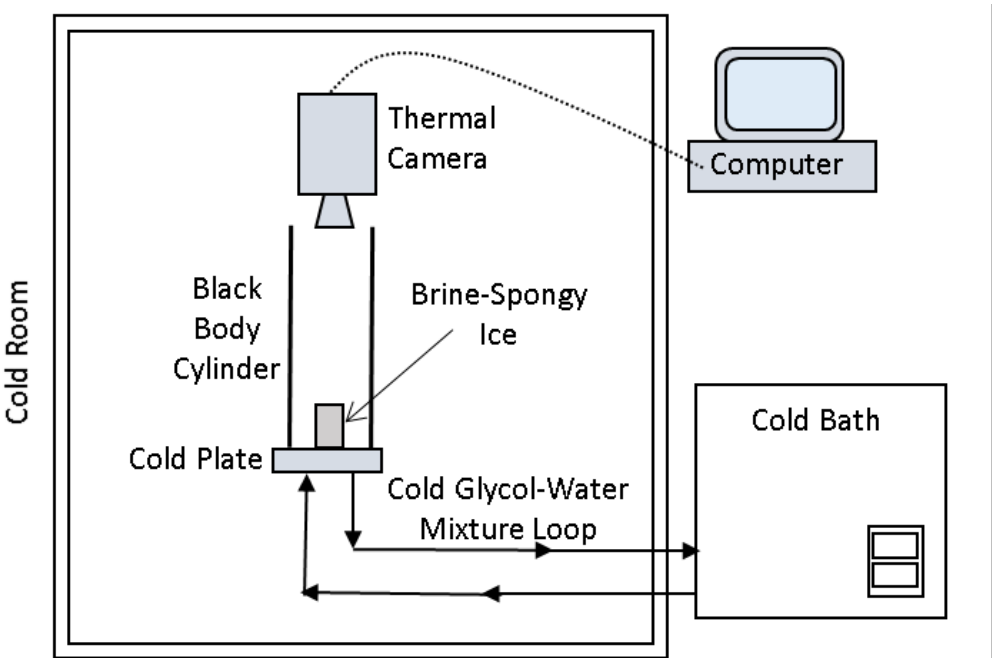

404

405 Fig. 5. Schematic of the experimental setup

406

407

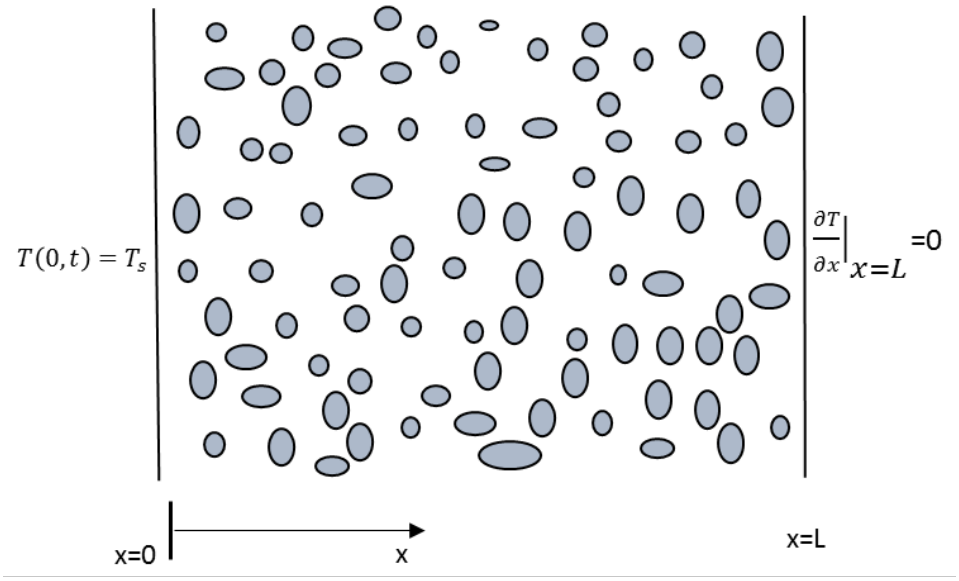

408

409 Fig. 6. Schematic of brine-spongy ice for the case study

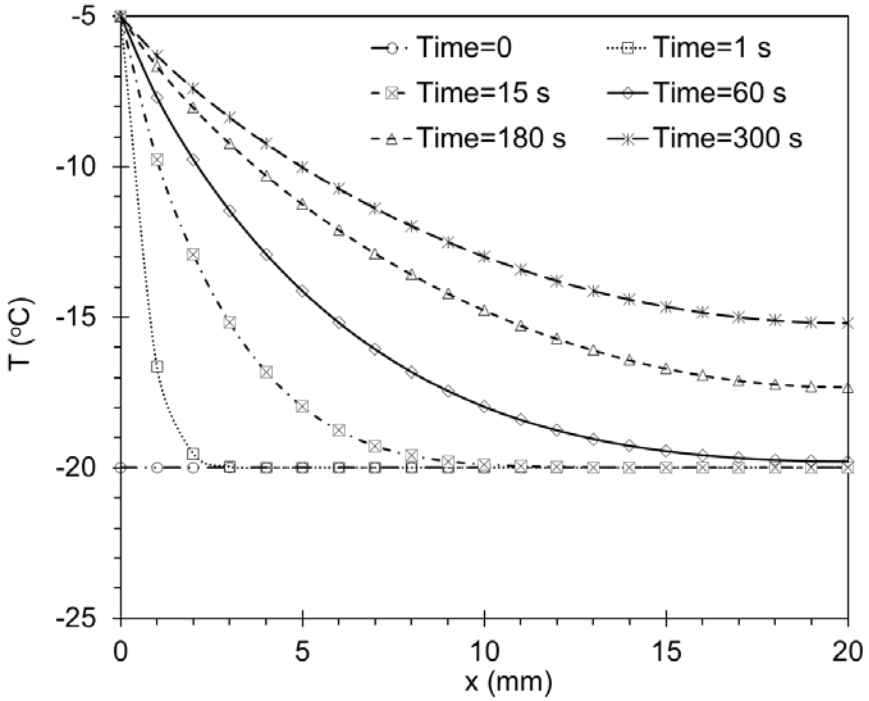

410

411 Fig. 7. Thermal response of brine-spongy ice

412

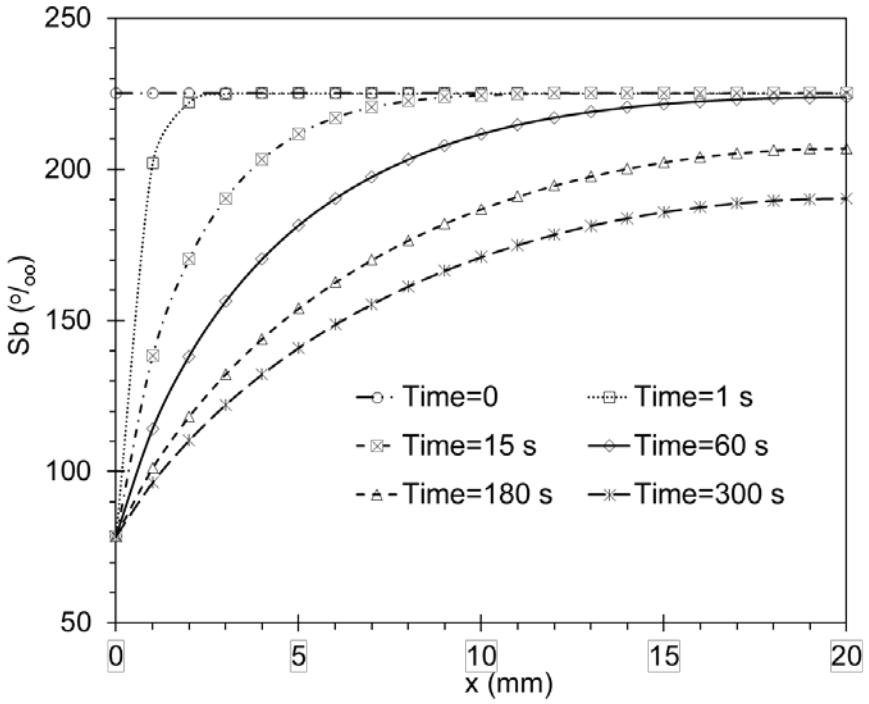

413

414 Fig. 8. Variation of salinity of brine pockets versus time

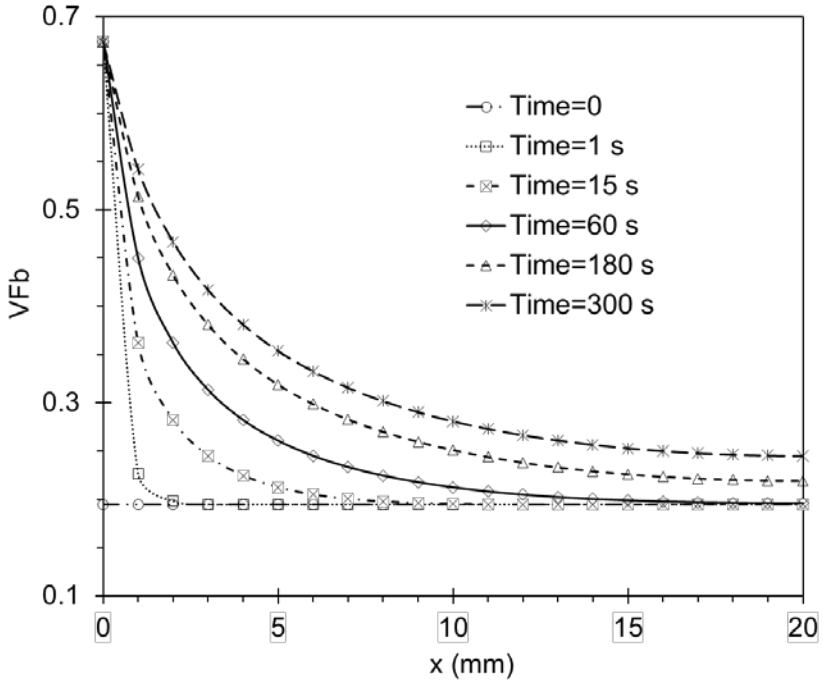

Fig. 9. Variation of volume fraction of brine pockets versus time

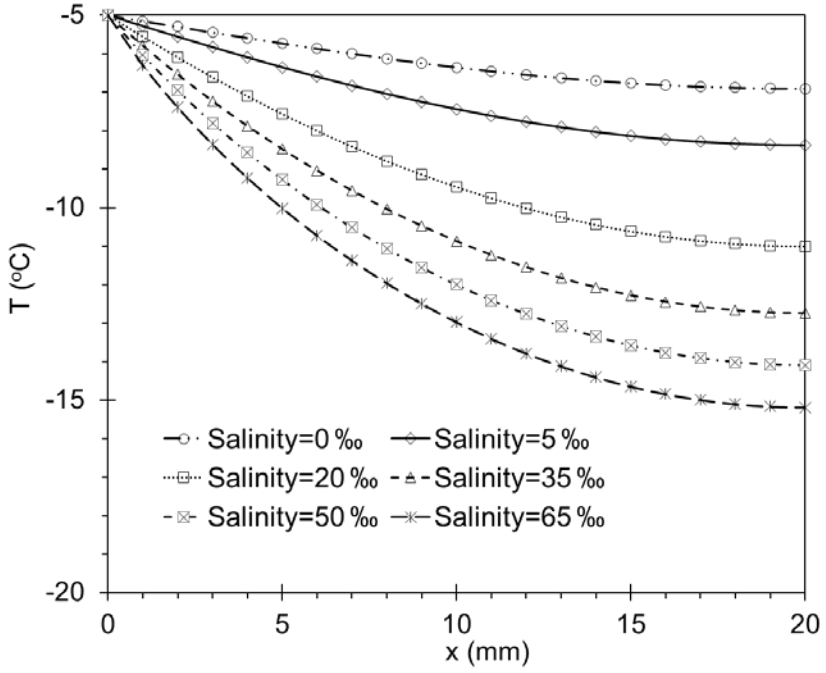

Fig. 10. Temperature variation of brine-spongy ice versus overall salinity

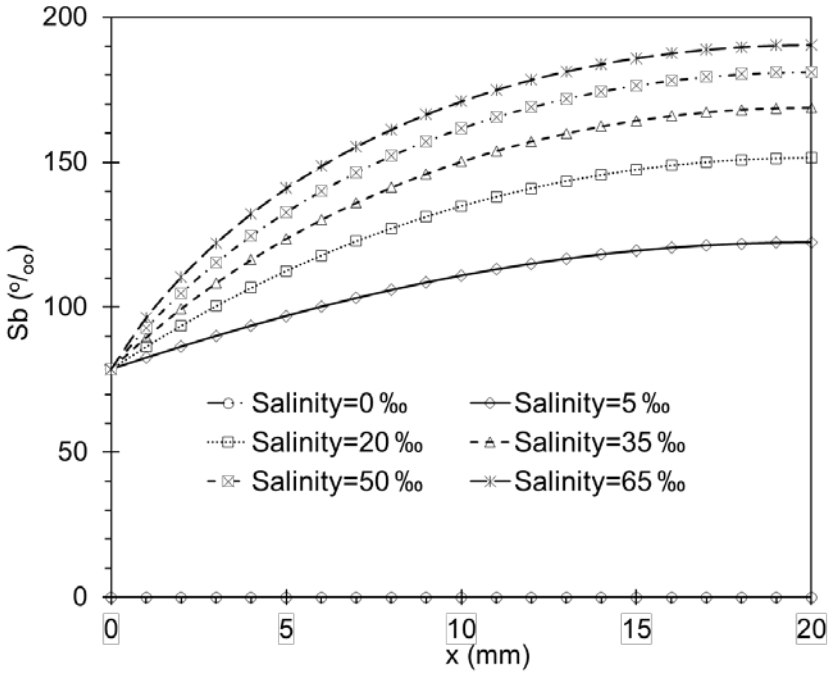

Fig. 11. Variation of salinity of brine pockets versus variation of overall salinity

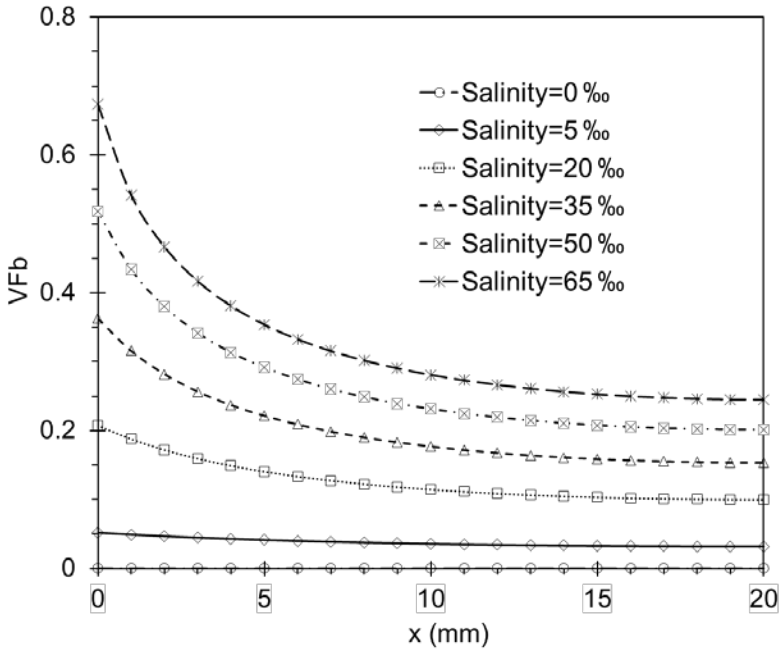

Fig. 12. Variation of brine volume fraction versus overall salinity

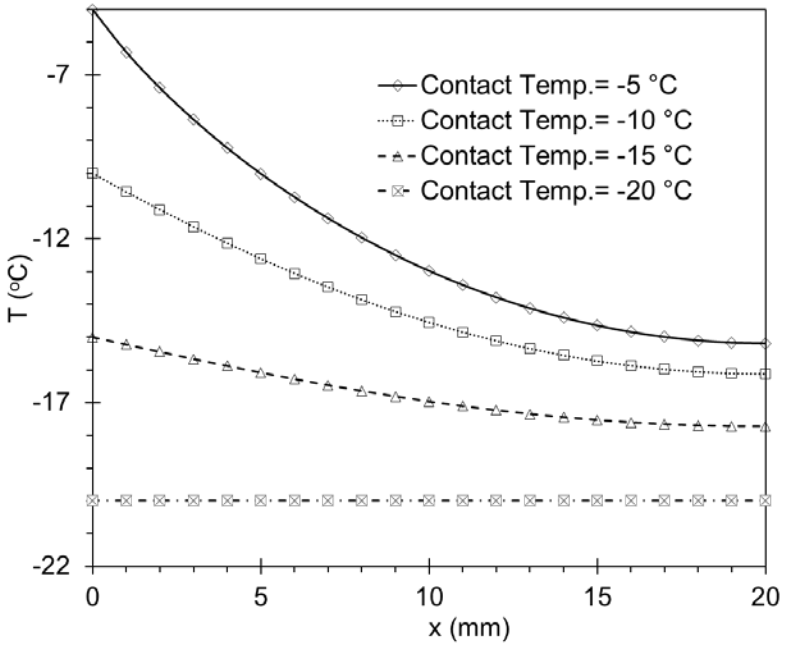

Fig. 13. Effects of contact temperatures on variation of temperature in brine-spongy ice

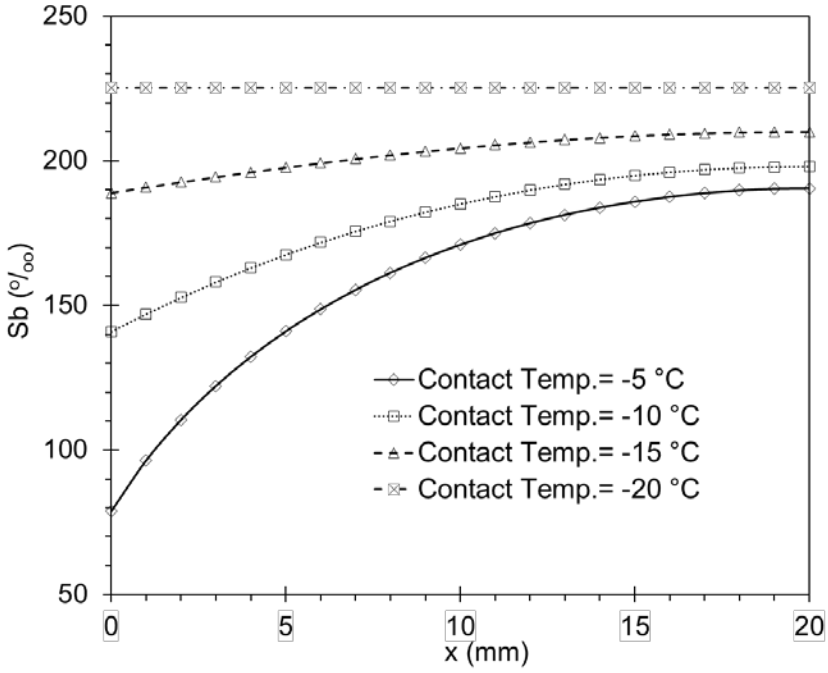

Fig. 14. Variation of salinity of brine pockets versus contact temperatures

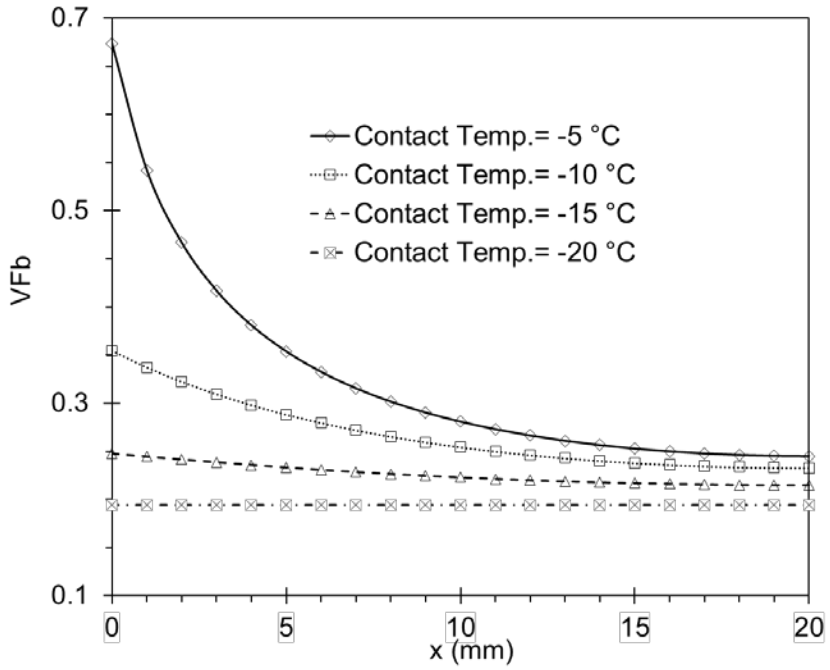

Fig. 15. Variation of volume fraction of brine versus contact temperatures

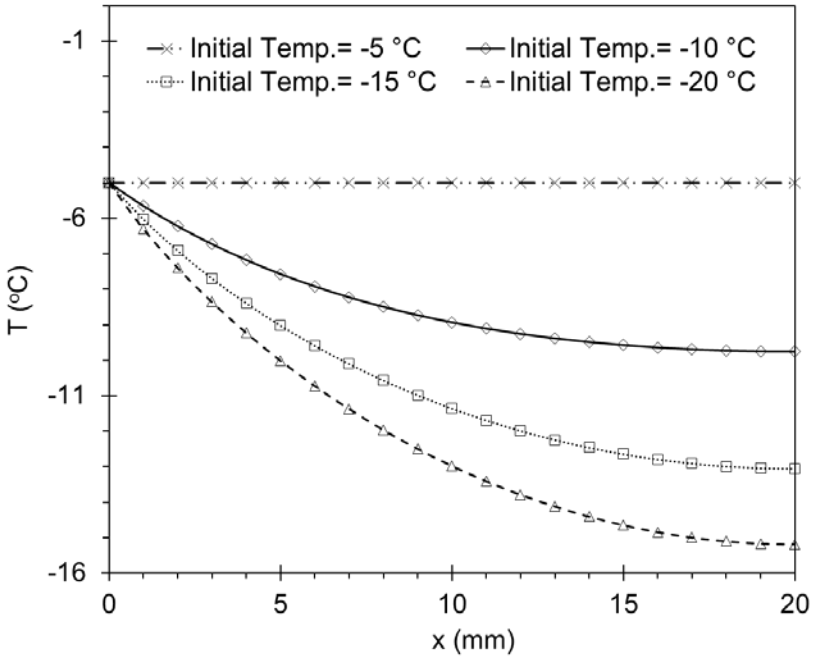

Fig. 16. Thermal response of brine-spongy ice in different initial temperatures

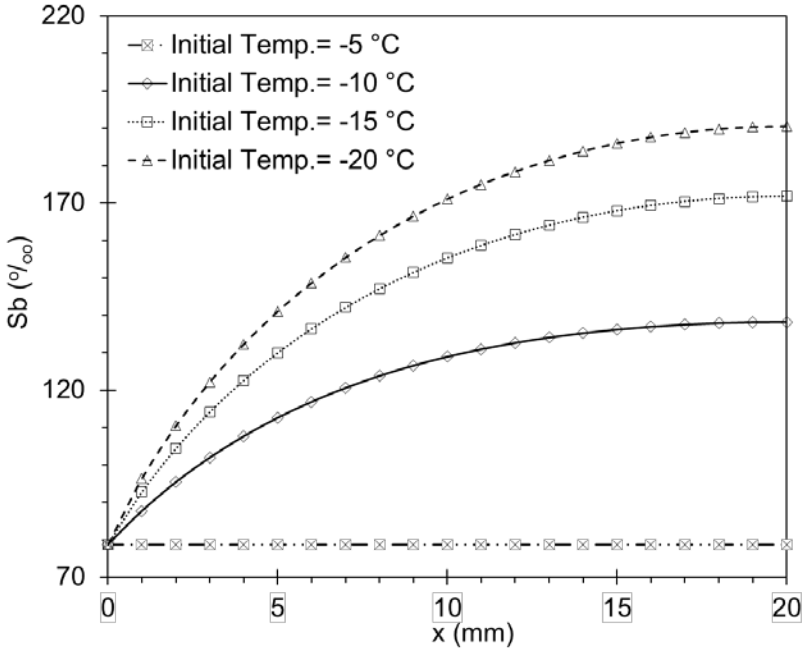

Fig. 17. Variation of salinity of brine pockets in various initial temperatures

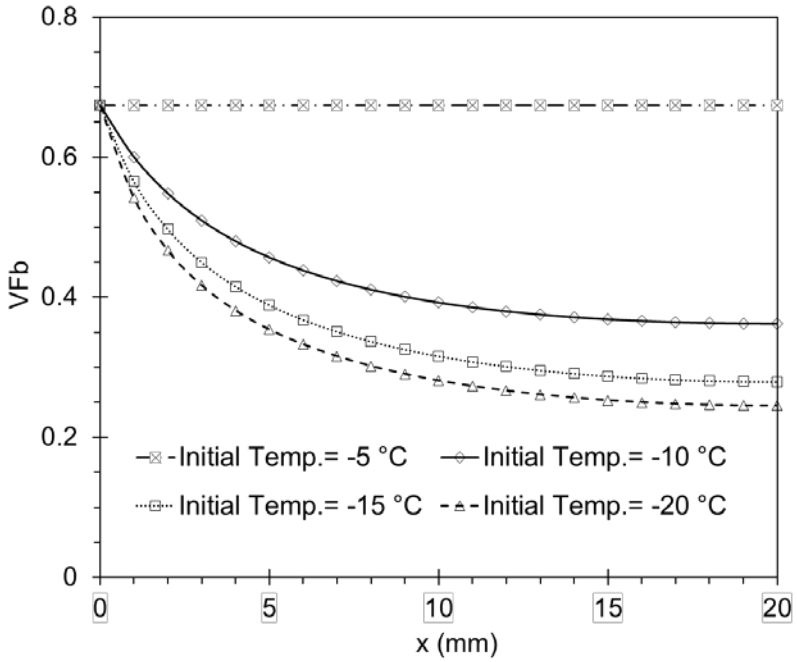

Fig. 18. Variation of volume fraction of brine in various initial temperatures

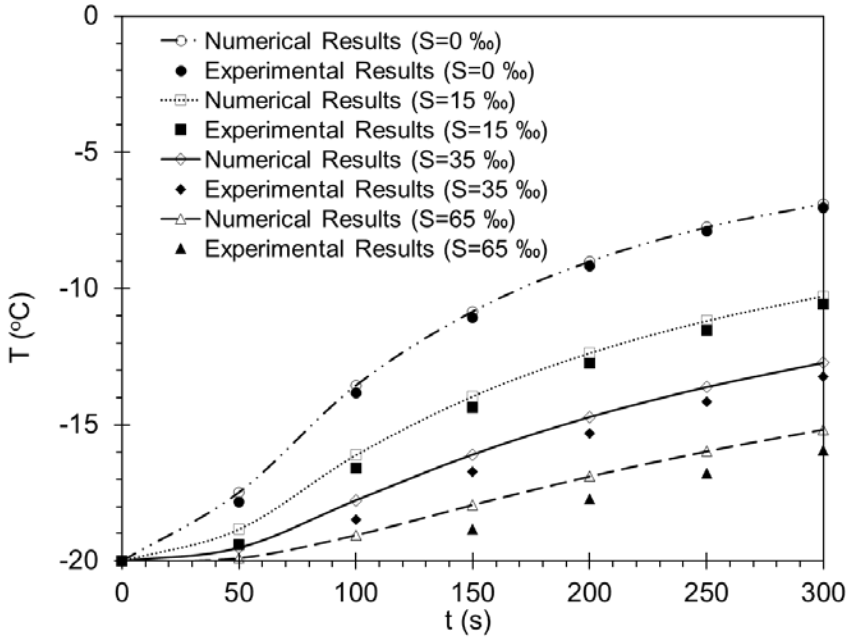

Fig. 19. Experimental and numerical results of temperature of brine-spongy ice block at various overall salinities

Table 1. Properties of ice, brine, and brine-spongy ice

Properties	Equations
S_b	$\alpha_{Sb1}\,T + \alpha_{Sb2}\,T^2 + \alpha_{Sb3}\,T^3$
ρ_b	$\alpha_{\rho b0} + \alpha_{\rho b1}\,S_b$
L_{Hb}	$\alpha_{LHb0} + \alpha_{LHb1}\,T + \alpha_{LHb2}\,T^2$
C_b	$\alpha_{Cb0} + \alpha_{Cb1}\,T + \alpha_{Cb2}\,T^2 + \alpha_{Cb3}\,T^3$
k_b	$\alpha_{kb0} + \alpha_{kb1}\,T + \alpha_{kb2}\,T^2$
ρ_i	$\alpha_{\rho i0} + \alpha_{\rho i1}\,T$
C_i	$\alpha_{Ci0} + \alpha_{Ci1}\,T$
k_i	$\alpha_{ki0} + \alpha_{ki1}\,T$
k_s	$k_b\,V_{Fb} + k_i\,(1 - V_{Fb})$
ρ_s	$\rho_b\,V_{Fb} + \rho_i\,(1 - V_{Fb})$
C_s	$C_b\,V_{Fb} + C_i\,(1 - V_{Fb})$

Table 2. Coefficients for equations of properties

Coefficients	Values			
	(0)	(1)	(2)	(3)
$\alpha_{Sb()}$	0	-17.5730	-0.381246	-3.28366×10^{-3}
$\alpha_{LHb()}$	-333400.326	-4958.217	-29.894	0
$\alpha_{\rho b()}$	1000	0.8	0	0
$\alpha_{Cb()}$	4211.249	111.437	5.125	93.545×10^{-3}
$\alpha_{kb()}$	0.5664	3.0822×10^{-3}	1.8388×10^{-5}	0
$\alpha_{\rho i()}$	917	-0.1403	0	0
$\alpha_{Ci()}$	2118.5199	7.8000	0	0
$\alpha_{ki()}$	2.2399	-10.7517×10^{-3}	0	0